Article

J. Mex. Chem. Soc. **2019**, *63*(1)

ISSN-e 2594-0317

Effect of the thermal annealing on the phase transitions of biogenic $CaCO_3$ nanostructures

Ramón-De los Santos Candelario[1], López-Rodríguez Angélica Silvestre[1], Sifuentes-Gallardo Pio[1], Hernández-Rivera Miguel Ángel[1], Pérez-Hernández German[1], Garnica-Romo Ma. Guadalupe[2], Rivera-Trejo José Guadalupe Fábian[1] and Díaz-Flores Laura Lorena[1*]

[1]Universidad Juárez Autónoma de Tabasco, Avenida Universidad S/N, Zona de la Cultura, Col. Magisterial, 86040, Villahermosa, Centro, Tabasco, México
[2]Universidad Michoacana de San Nicolás de Hidalgo, Santiago de Tapia 403, 58000 Centro, Morelia, Michoacán, México.

***Corresponding author:** Díaz-Flores Laura Lorena, laura.diaz@ujat.mx +52 914 105 7150

Received December 2nd, 2018; Accepted Janaury 22nd, 2019.

DOI: http://dx.doi.org/10.29356/jmcs.v63i1.422

Abstract. The issue of the present research lays its foundation on the proposal of the *Crassostrea virginica* waste oyster shells (WOS) reuse to obtain calcium carbonate powder ($CaCO_3$) and calcium hydroxide ($Ca(OH)_2$) nanostructured, using thermal annealing treatments. The oysters shells were subjected to a previous physical grinding process to decrease their size (smaller sizes 0.074 mm). The parameter studied was the effect of annealing temperature (500, 700 and 900 °C in air atmosphere) on the structural properties and morphology of the powders by FTIR, XRD, SEM and HRTEM. The X-ray diffraction results indicate that the WOS in their natural state and thermally annealed at 500 °C have two phases of $CaCO_3$ the rhombohedral form for calcite with crystallite size around 24 nm and aragonite traces in orthorhombic phase. At 700 °C, the WOS powder is transformed into calcium hydroxide, also known as portlandite ($Ca(OH)_2$), attributed to the absorption of water released during the thermal decomposition of $CaCO_3$. This crystalline phase does not change when the temperature increases to 900 °C. The SEM and HRTEM analysis of WOS powders reveals that with a thermal annealing treatment it is possible to obtain nanostructured $CaCO_3$. FTIR analysis demonstrates the biogenic origin of $CaCO_3$, due to amide groups. The nanostructured $CaCO_3$ obtained by grinding and thermal annealing of WOS, can be used as drying agent, or as additive in ceramic and glass.
Keywords: Calcite; aragonite and portlandite; $CaCO_3$ rhombohedral nanostructure; $(Ca(OH)_2)$ hexagonal phase; $CaCO_3$ biogenic compound.

Resumen. El objetivo de esta investigación, es el reúso de desechos de conchas de ostión (WOS), para obtener polvos de carbonato de calcio ($CaCO_3$) e hidróxido de calcio ($Ca(OH)_2$) nanoestructurados, utilizando tratamientos térmicos en atmósfera de aire (500, 700 y 900 °C). Previamente a los procesos térmicos, las conchas de ostión fueron sometidas a un proceso de molienda para decrecer su tamaño (Tamaños menores a 0.074 mm). El efecto del tratamiento térmico en las propiedades estructurales y morfológicas de los polvos de WOS se analizaron por FTIR, DRX, SEM Y HRTEM. Los resultados de Rayos X indican que los polvos de WOS en sus estados natural y tratados térmicamente contienen dos fases cristalinas de $CaCO_3$: la forma romboédrica para la calcita, con un tamaño de cristalito de aproximadamente 24 nm y trazas de aragonita en la fase ortorrómbica. A 700 °C los polvos de WOS se transforman a hidróxido de calcio ($Ca(OH)_2$), también conocido como portlandita, atribuido a la absorción de agua durante la descomposición térmica del $CaCO_3$. Esta forma cristalina no cambia por efecto de incrementar la temperatura a 900 °C. Los análisis de SEM y HRTEM, revelan que con un tratamiento térmico a los polvos de WOS es posible obtener $CaCO_3$ nanoestructurado. Los análisis de FTIR, corroboran el origen biogénico del $CaCO_3$, por la

J. Mex. Chem. Soc. **2019**, *63*(1)

ISSN-e 2594-0317

presencia de los grupos amidas. El $CaCO_3$ nanoestructurado obtenido por molienda y tratamientos térmicos de los WOS, puede ser utilizado como agente secante o aditivo.
Palabras clave: Calcita; aragonita; portlandita; Nanoestructuras romboédricas de $CaCO_3$; Fase hexagonal de $Ca(OH)_2$; Compuesto biogénico de $CaCO_3$.

Introduction

The oyster shell is a natural resource, that after consumed as food, is completely wasted since most of the people think the inner content is all that this *Crassostrea virginica* mollusk offers. However, oyster shells contain high amounts of calcium carbonate, calcium oxide and calcium hydroxide [1]. All these compounds are very useful for the preparation of building materials [1], the restoration of contaminated soils [2], water purification [3], and building restoration [4]; even in commercial products like nutritional supplements of calcium-based oyster shell. The above mentioned calcium compounds have complex and pre-ordered structures with good mechanical and chemical properties, therefore, several investigations have been conducted towards obtaining $CaCO_3$ nanoparticles by chemical synthesis [4-5], and their potential applications.

The calcium carbonate ($CaCO_3$) is a compound insoluble in water, contained in minerals such as calcite, dolomite and aragonite, and their applications include drying agents, or as additives in ceramic and glass; in all cases it is used in ultrafine sizes. Regarding this matter, Chen et al [6], obtained a smaller particle of 94 nm with a narrower distribution of $CaCO_3$ mineral using a low rotation speed in a planetary ball mill. Nowadays, with the scientific discoveries in nanotechnology area, it is possible to develop new materials with nanometric sizes and compositions adapted to current needs in technological devices, medicine, food etc Bastida *et al* in their research evaluated the kinetics of $CaCO_3$ decomposition by thermal treatments and performed a microstructural analysis using the X-ray technique, finding crystallite sizes of the order of 100 nm [7]. In addition, recent research reported the impact of synthesizing nanoparticles of $CaCO_3$, from a reactor with emulsions prepared from an experimental design and controlled processes [8]. Other authors point out the use of the $CaCO_3$ in emulsion, as an efficient antimicrobial agent against the *Staphylococcus aureus* (S. aureus) [9]. As well as an antimicrobial, it is used in foods under the function of a nanomaterial that traps the aromatic molecules of food and preserves its aroma for longer periods [10]. These applications are possible due to the increase of surface area with nanoparticles of the $CaCO_3$.

Furthermore, calcium hydroxide obtained by waste oyster shells calcined at 1000 ºC, has been reported as improving water quality, where the calcined oyster shells powder plays a key role as CO_2 adsorbent by measuring the removal efficiency for algal blooms in algae-containing water [11]. As well as, this $Ca(OH)_2$ has been obtained by a chemical precipitation method in an aqueous medium at 90 °C using waste oyster shells and this product was denominated by the authors as eco-friendly Green Calcium Hydroxide Nano-plates (GCHNPs)[12]. Weiner *et al* [13] reported that biominerals are formed from a precursor amorphous produced from saturated solutions, which are then transformed into its crystalline phase. With regarding to the calcium carbonate, subsequent studies, reporting even the study of the polyamorphism of this compound and its role in biomineralization [14]. In related works, but with another type of mollusk the *Periglypta magnificaI*, it was found that the soluble and insoluble protein controlled its crystalline structure and the mineralization process. In this work, the annealed treatment was 80 °C and the aragonite phase was found in the nacreous layer (internal) and calcite in the external part of the shell [15]

For oyster shells powder Chiou *et al* reports the transformation of these in three main crystalline species, $CaCO_3$, CaO, and $Ca(OH)_2$ in un-calcined oyster shells the crystalline form was $CaCO_3$, following with thermal treatment at 550–750 ºC, while after calcining at 750 ºC, the CaO was obtained. For oyster shells calcined, the main specie was CaO, which easily reacts with ambient humidity to form $Ca(OH)_2$, which made calcined oyster shells strongly alkaline [16]. The currently interest of using this type of biogenic source is because at that several investigations have focused on using physicochemical properties of these materials derived from powders of oyster shells as adsorbents for heavy metals such as Cd, Pb and Cu. Which have already been tested in our previous work reported [17], where the aim of that study was evaluate the adsorption capacity of biogenic $CaCO_3$ nanostructures in the presence of metal ions (Cd^{2+} and Cu^{2+}) in aqueous solutions. In this research, we presented the results of the physical-chemical characterization of biogenic $CaCO_3$ nanostructures. Furthermore based on the coefficients of adsorption (Kd) and the values of percentage of metal removed, the metals selectivity sequence is cadmium (II) > copper (II) to be adsorbed by $CaCO_3$ nanostructures. Considering the current interest in the development of green chemistry using waste materials for the synthesis of biogenic nanomaterials, we collected and analyzed waste oyster

J. Mex. Chem. Soc. **2019**, *63*(1)

ISSN-e 2594-0317

shells (WOS) from the coastal zone of Tabasco, Mexico. To synthesize biogenic calcium materials, WOS were collected, washed and grinded, prior to their subjection to thermal treatment. To evaluate the effect of the thermal annealing, in the shape and size of the particles of calcium carbonate, the structural and morphological characterizations were done by FTIR, XRD, SEM and HRTEM.

Experimental

Methods

Preparation of powder samples from waste oyster shells (WOS)

WOS were collected in the coastal area of Tabasco, a state located in the southeast of Mexico, in the Gulf of Mexico. Impurities adhered to shells were cleaned off with water and a sponge. Then, the shells were broken into small pieces with a hammer and subjected to the mechanical grinding in a ball mill equipment at 100 rpm for one hour. After this, 100 g of the milled powder was separated and left in natural state (WOS-WT) and 300 g were subjected to annealing thermal treatments (100 g for each sample) at 500 °C (WOS-500 °C), 700 °C (WOS-700 °C) and 900 °C (WOS-900 °C) with a ramp heating of 10 °C min^{-1} and times of 4 hours in a furnace at atmospheric conditions. Once all powders were sintered, they were sieved through a 200-sized mesh to obtaining homogeneous-sized particles and some others under 0.074 mm.

Characterization techniques and measurement methods

Throughout the procedure, all the calcium powders with and without thermal treatment were analyzed in structure and morphology. Structural analysis by FTIR was performed using a Shimadzu spectrometer. The spectra were measured in a wavelength range of 600-4000 cm^{-1}, with resolution of 2 cm^{-1} and 40 scans. WOS powders were analyzed with a Rigaku X-Rays Diffractometer, with 1,544 Å wavelength, applying Cu kα radiation, to determine the existence of the crystalline phase. For morphological characterization of WOS, a field emission scanning electron microscope was used (FE-SEM) JSM-7100F, with 2 kV of accelerating voltage under vacuum conditions. Nanocrystalline size was determined by HRTEM. HRTEM measurements were carried out with HRTEM JEOL JEM-2100 200 kV. Powders samples of WOS, were sonicated for 15 min in acetone, and then drop deposited onto copper grids of 200 mesh squares, diameter 3.05 mm supported onto TEM holder.

Results and discussion

The results of the percentage of yield of the powders WOS submitted to the thermal treatments were of 67%. Yong *et al* found that calcination under an air atmosphere leads to a mass loss of 45%, which was comparable to the calcination results observed in the present study with 33% weight loss (Fig. 1) [18]. In the same way, the analysis of the amount of powders passing through 200-sized meshes (0.074 mm) is presented as % sieved mass, and it is possible to observe that with increases in thermal treatment , the % sieved mass increase. This could be due to sieve openings tend prone to blinding, by particles with sizes of similar diameter, so it was necessary to carry out additional examination for the particles with another method of measurement (HRTEM).

J. Mex. Chem. Soc. **2019**, *63*(1)

ISSN-e 2594-0317

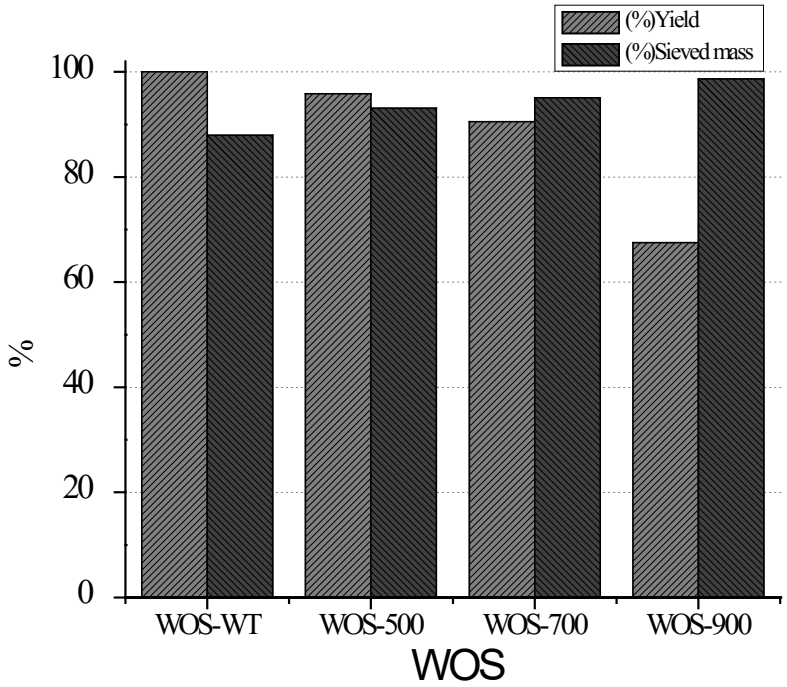

Fig. 1. Percentage of yield and final amount of WOS powders after thermal annealing

Analysis by FTIR

Fig. 2 shows four FTIR spectra in a range of 600 to 4000 cm^{-1} in absorbance mode and they correspond to powder from natural shell (WOS WT), annealed powders shell (WOS 500 °C, WOS 700 °C and WOS 900 °C). In all spectra, the main and most intense signal appears at 1500 $cm^{-1,}$ and the second band appears at 886 cm^{-1}. These bands are associated with vibrations for the functional group of the νC=O in stretching mode. The analysis of the spectrum corresponding to raw oyster shells (WOS WT) indicate the presence of different absorption bands associated with functional group C=O mainly at 715, 845, 1470 cm^{-1} [19]. In addition, in this spectrum it is also possible to observe bands associated with the following groups: N-H in 3500 cm^{-1}, C-H in 2838 cm^{-1}- 3000 cm^{-1}, S-H in 2500 cm^{-1}, amide type I in 1780 cm^{-1} and amide type II in 1500 cm^{-1}. All of these latest vibrations are attributed to a specific fingerprint of compounds of biological origin [3], so it is assumed that a protein which formed the nacre of the oyster shell calcium carbonate, still remains in the structure. Evaluating the effect of the thermal treatment at 500 °C, it is observed that spectrum retains bands associated with group C=O, S-H and C-H, but with greater intensity and better definition of absorption bands; however, bands associated with absorption of N-H group disappear. After subjecting WOS powders to thermal treatment at 700 °C and 900 °C consecutively, and analyzing them by infrared spectroscopy, it can be observed that vibrations associated with carbonyl groups remain visible. Nevertheless, in 3450 cm^{-1}, it reveals a band associated with $Ca(OH)_2$, which is attributed to the absorption of the humidity of the environment [20]. As a result of the spectroscopic analysis, it was determined that the samples of powder oyster shells without treatment (WOS-WT) and with WOS 500 °C, preserve their structure of calcite with the presence of an absorption band at 713 cm^{-1} [21].

By using band assignments from literature [22-23], it is possible to infer that calcium carbonate has polymorphism: calcite or aragonite. Therefore, using the band deconvolution method in WOS-WT and WOS 500 spectra, in the region of 665 to 740 cm^{-1} (Fig. 3), it was possible to observe that in the first one there are two phases: calcite to 713 cm^{-1}, and aragonite to 700 cm^{-1}. For WOS 500 °C, the band associated to calcite increased and aragonite decreased.

J. Mex. Chem. Soc. **2019**, *63*(1)

ISSN-e 2594-0317

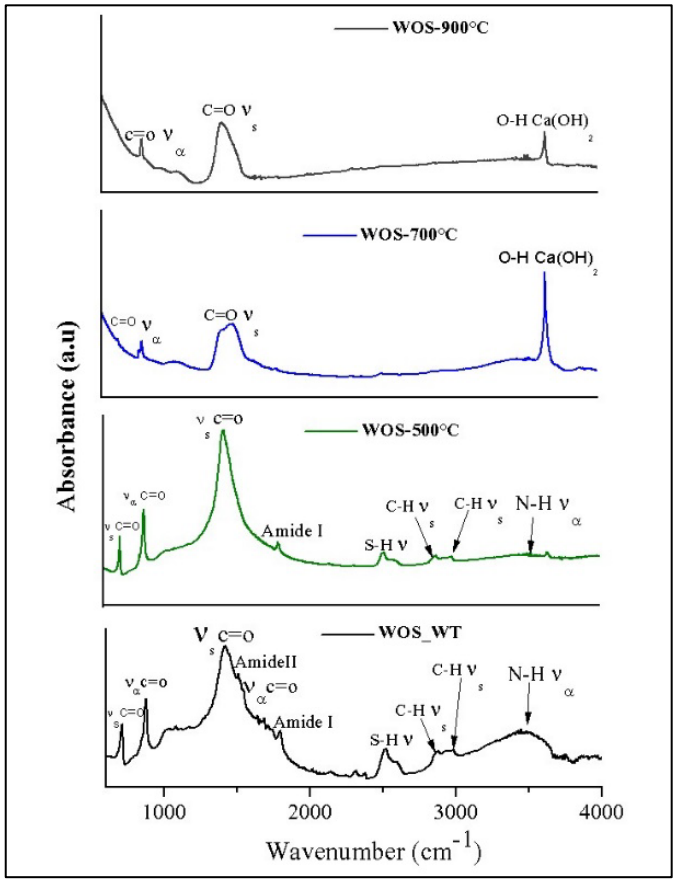

Fig. 2. FTIR spectra for WOS powders without thermal treatment (WOS WT), and thermal annealing at 500 (WOS-500 °C), 700 (WOS-700 °C) and 900 °C (WOS-900 °C).

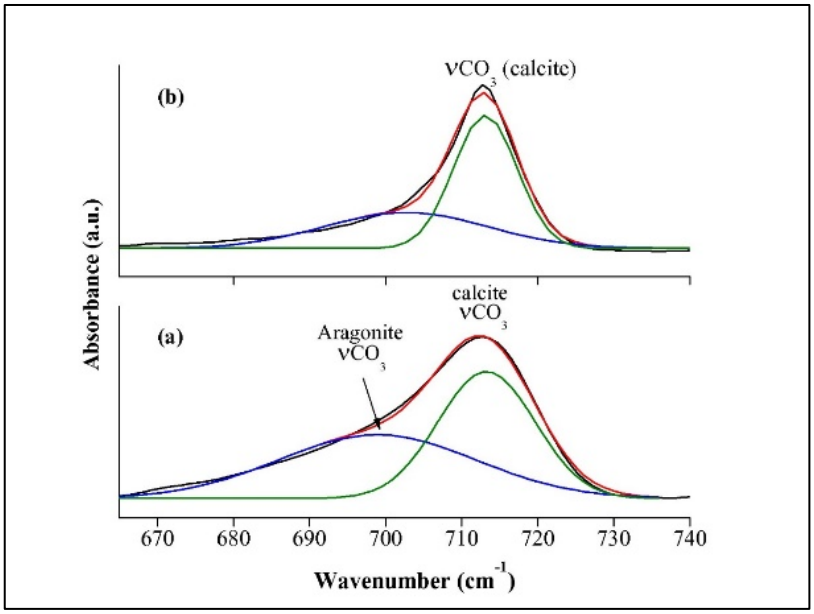

Fig. 3. FTIR Deconvolution of υCO3 band (665—740 cm^{-1}) showing (a) calcite and aragonite for WOS-WT and (b) the evolution of aragonite to calcite in WOS-500 °C.

J. Mex. Chem. Soc. **2019**, *63*(1)

ISSN-e 2594-0317

Analysis by DRX

Crystal structures of WOS powders were analyzed by X-ray diffraction. Results agree with those previously obtained by infrared spectroscopy. Fig. 4, shows the effect of thermal treatment in structural changes of the powders components with the X-ray diffractograms in 2θ range of 10 to 80 º. Analyzing all diffractograms for WOS-WT and WOS-500 °C, it is observed that both patterns show the same peaks in position and nearly the same intensity to the planes of reflection patterns to calcite ($CaCO_3$), (104 and 108) and (106) in 29°, 38° and 39° 2θ, respectively. As the waste oyster shell powders are subjected to higher temperature 700°C and 900°C (in air atmosphere), they suffer a transformation from calcium carbonate to calcium hydroxide with crystal structure associated with the portlandite ($Ca(OH)_2$). Both patterns of diffraction WOS-700°C and WOS-900°C, present the same peaks, without changes in intensities of (001, 100, 101,002, 012, 110 and 111) reflections and are corresponding to database PDF (Portable Document Format) 01-076-0571. The decrease in the intensity of the peaks when the temperature changes from 700 to 900 ºC could be because of the conversion into Ca(OH)2 still begins, so at this temperature there is the possibility that a mixture of phases of calcite and portlandite and the preferential orientation of the diffraction peaks change intensity. With these results, it was possible to determine the presence of $CaCO_3$ in form of calcite in the natural oyster shells and thermally treated at 500 °C. In addition, in the samples with thermal treatment at 700 °C and 900 °C, $Ca(OH)_2$ appears in the shape of portlandite. For this particulate case of $Ca(OH)_2$, it is complicated to quantify the amount of water absorbed during the change of phase, which makes it an unstable phase and the result of Scherrer´s equation would be imprecise. For the calculation of the particle size of the $Ca(OH)_2$, a more detailed analysis is recommended using the method of analysis of Rietveld diffraction patterns.

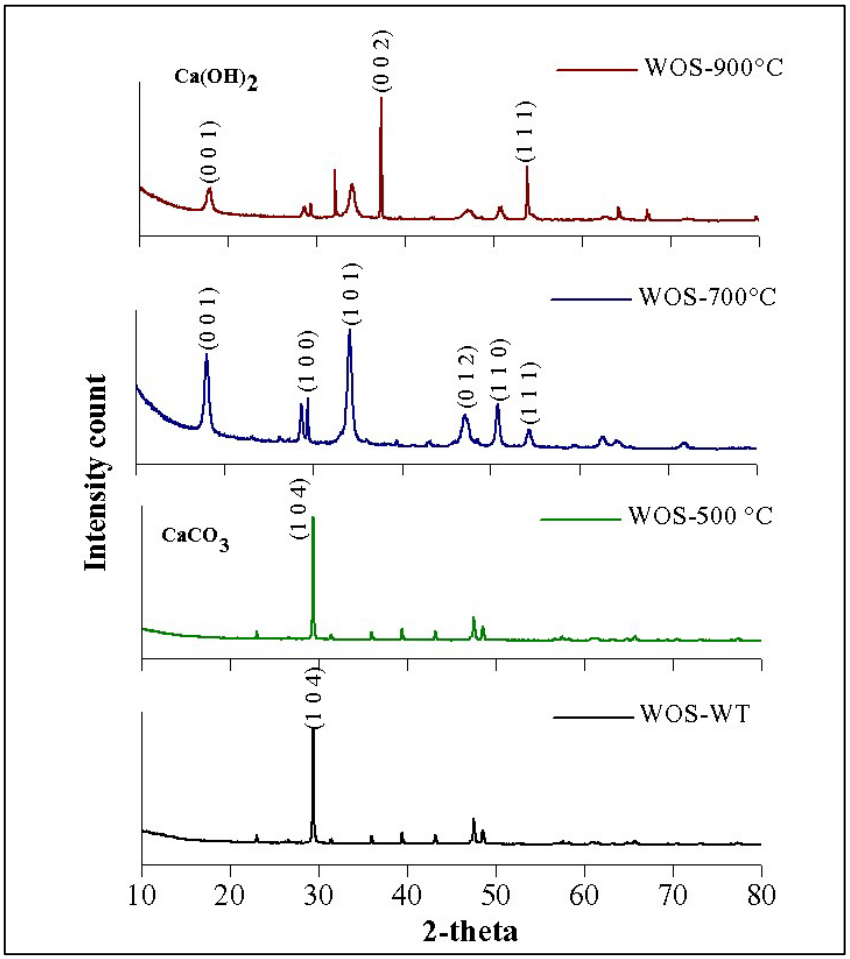

Fig. 4. XRD patterns for WOS powders without thermal treatment (WOS WT); and thermal annealing at 500 (WOS-500 °C); 700 (WOS-700 °C) and 900 °C (WOS-900 °C).

J. Mex. Chem. Soc. **2019**, *63*(1)

ISSN-e 2594-0317

To approach the particle size (D) for $CaCO_3$ crystals, we use Debye - Scherrer equation (Ec. 1):

$$D = \frac{0.9\lambda}{B\cos\theta} \qquad \text{Ec. (1)}$$

where: λ, is X-ray wavelength (1.5418 Å); B, is the full width at the half-maximum of the $CaCO_3$ (104) line and θ is the diffraction angle, resulting in a crystal size of the order of 24 nm. In addition to the carbonate of calcium in form of calcite, it also presents aragonite traces, another type of carbonate of calcium but with different crystal structure. Fig. 5 shows an onset of diffraction patterns WOS-WT (a) and WOS-500°C (b), where it was possible to identify two peaks corresponding to: aragonite, (letter A) and calcite, (letter C). All diffraction peaks correspond to calcium carbonate in two crystalline forms: the calcite type (rhombohedral) [24] and the aragonite type (orthorhombic) (Fig. 5a) [4]. When the aragonite is heated up, it changes its crystalline structure into calcite (Fig. 5b), as described by Yoshioka and Kitano [2], who assumed that this transition phase may be due to the amount of water present in the structure of aragonite and this plays an important role in phase transition. The analysis of diffractograms reveals that the rhombohedral calcite prevails in the WOS-WT and WOS-500 samples, according to the PDF 00-047-1743, as it overtakes the orthorhombic phase (PDF 01-083-0577) in WOS -500 °C powder, coinciding with space and intensities of published powder diffraction patterns.

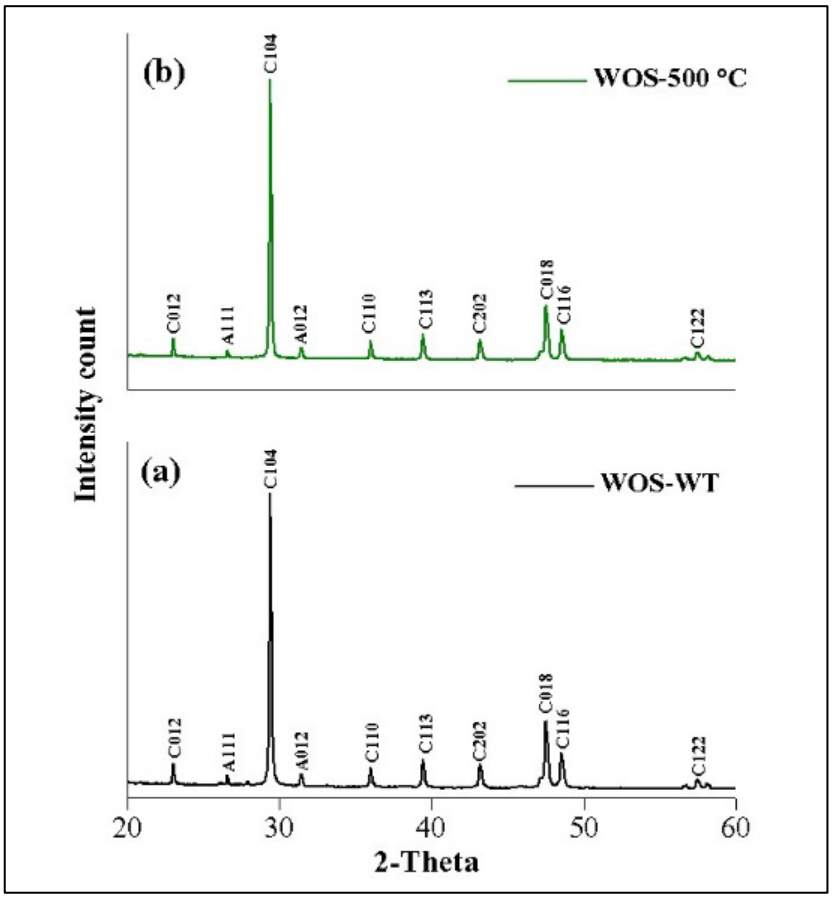

Fig. 5. XRD patterns for (a) calcite in rhombohedral form (PDF 00-047-1743) in the WOS-WT powder and (b) calcite orthorhombic (PDF 01-083-0577) in WOS -500°C powder.

J. Mex. Chem. Soc. **2019**, *63*(1)

ISSN-e 2594-0317

Characterization by SEM

A SEM morphological analysis, with a scale of 1 μm and 5000 X, is represented in Fig. 6. The images correspond to samples of WOS powders: natural (a), annealed thermal to 500°C (b), 700 °C (c) and 900 °C (d). The foliated structure of a natural sample (Fig. 6a), has different sizes of agglomerates, ranging from 0.5 μm to 2 μm. These powders are transformed by effect of the thermal annealing at 500 °C, grain sizes decrease to uniform sizes smaller than 500 nm (Fig. 6b). However, with thermal treatment at 700°C, grains grow and irregular shapes are observed (Fig. 6c). The same occurs in the sample of 900 °C, but with grain greater than 5 μm (Fig. 6d). These results coincide with those previously found by Hamester *et al* [5].

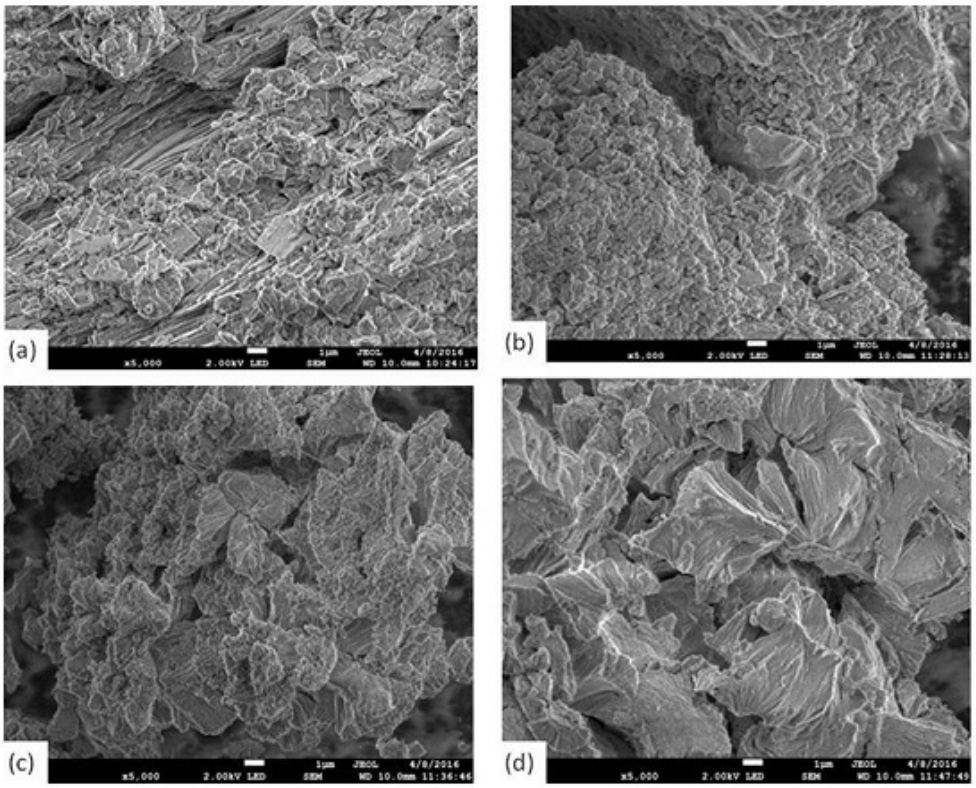

Fig. 6. Analysis by SEM of the effect of annealing treatment on the morphologies and grain size of WOS powders without thermal treatment (a); and thermal annealing at 500 °C (b); 700 °C (c) and 900 °C (d)

Analysis of the $CaCO_3$ phase transitions by HRTEM

As previously discussed in the characterization by FTIR and XRD, the compounds of $CaCO_3$ and $Ca(OH)_2$, obtained by mill and thermal treatments, are calcite, aragonite and portlandite in rhombohedral, orthorhombic and hexagonal crystalline phases, respectively. Fig. 7 shows the image in bright field by HRTEM, from the waste oysters shell powders subjected to different thermal treatments (a) without thermal treatment; (b) at 500 °C; (c) at 700 °C and (d) at 900 °C. In the images, three forms of particles can be seen at sizes smaller than 200 nm for the $CaCO_3$ (only milling and 500 °C) and bigger than 200 nm for 700 and 900 °C. As it can be observed in the images, in the case of $CaCO_3$ obtained from only milling, there are two crystalline structures: the orthorhombic and the rhombohedral, the first being of a bigger size than the second one. With heating treatment at 500 °C, rhombohedral-shaped particle decreases in size up to 50 nm. However, in the case of samples annealed at 700 and 900 °C, the composition changes to $Ca(OH)_2$, moreover, its structure turns into hexagonal, and particle size increases up to 400 nm.

J. Mex. Chem. Soc. **2019**, *63*(1)

ISSN-e 2594-0317

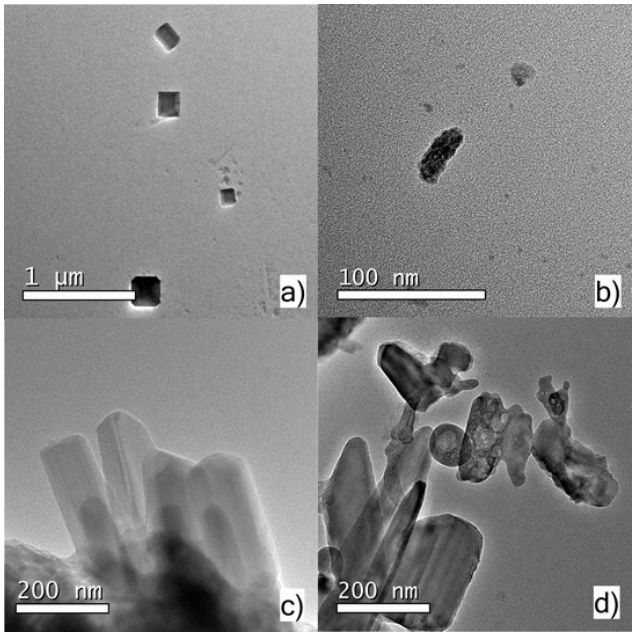

Fig. 7. Bright field HRTEM image of CaCO3 with particles dimensions ranging from 100–200 nm of WOS powders without thermal treatment (a); and thermal annealing at 500 °C (b); 700 °C (c) and 900 °C (d).

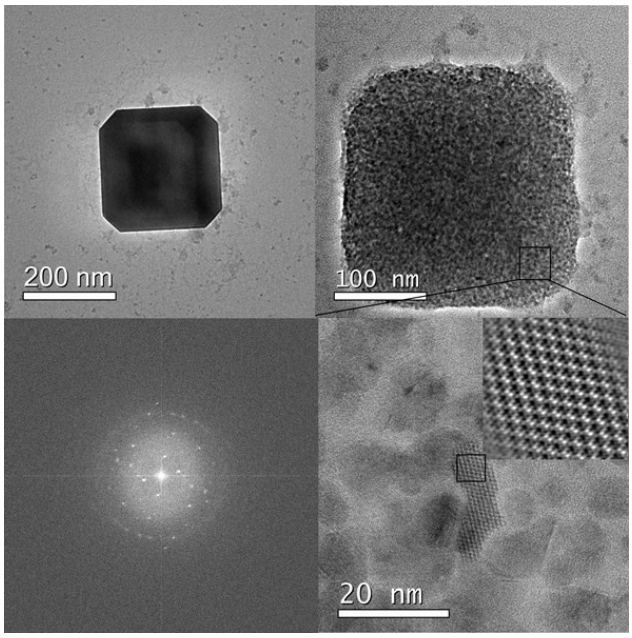

Fig. 8. HRTEM images of orthorhombic phase of $CaCO_3$ nanostructures and their corresponding diffraction pattern of WOS powders without thermal treatment.

In order to identify the crystal structure of the sample with only milling (WOS-WT), an area of 20 nm of the accumulated particle was selected (Fig. 8), and the diffraction pattern obtained is used for the orthorhombic phase of the $CaCO_3$. Comparing this image to the thermal annealed sample particle at 500 °C, it is evident that the nanoparticle diminished to 40 nm (Fig. 9). In this sample WOS-500 °C, two areas were selected, thus it is possible to identify the nano-crystalline rhombohedral and orthorhombic phases. It can be observed that, although the

J. Mex. Chem. Soc. **2019**, *63*(1)

ISSN-e 2594-0317

diffraction pattern shows a higher temperature, it contains more intense spots. Therefore, it is clear that the sample that has only gone through milling process contains particles larger than those in the 500 °C sample. In the third transition, from $CaCO_3$ to $Ca(OH)_2$, the nanoparticles size increased to around 500 nm and the diffraction pattern showed hexagonal phase attributed to the portlandite (Fig. 10).

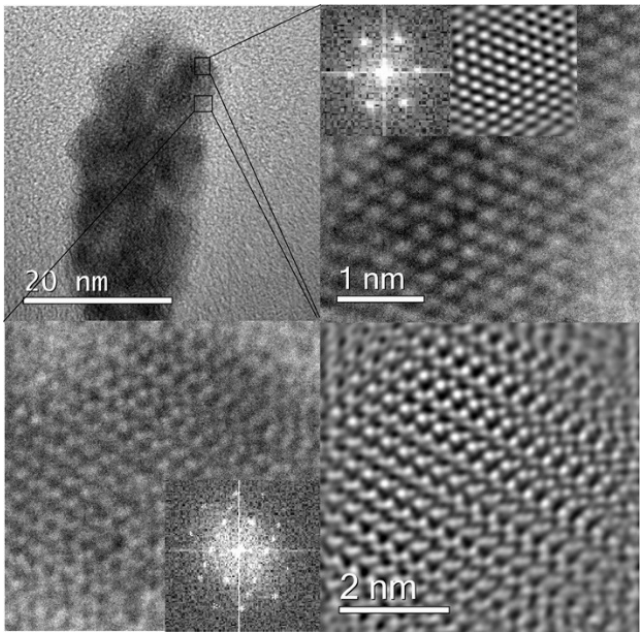

Fig. 9. HRTEM images of rhombohedral phase of nanostructured $CaCO_3$ acquired at different zone axes and their corresponding diffraction patterns of powders thermal annealing at 500 °C (WOS- 500°C).

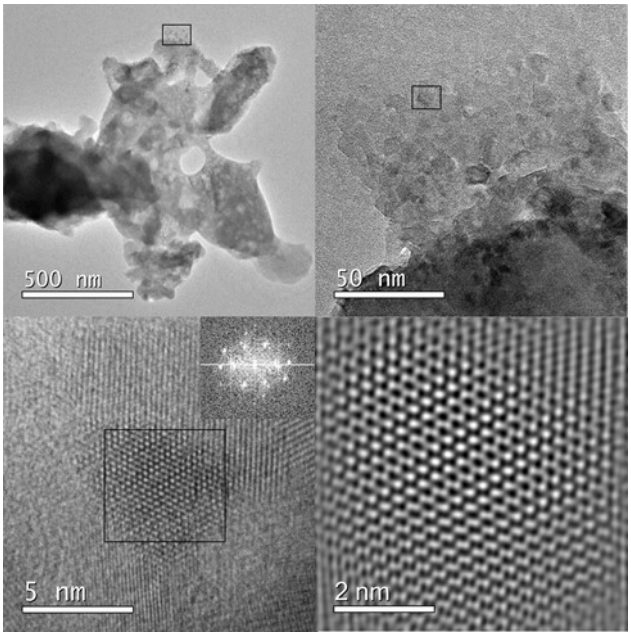

Fig. 10. HRTEM images of hexagonal phase of nanostructured $Ca(OH)_2$ and their corresponding diffraction pattern of WOS- 700°C.

J. Mex. Chem. Soc. **2019**, *63*(1)

ISSN-e 2594-0317

Conclusions

The $CaCO_3$ of the waste oyster shells (WOS) of seawater lagoons coastal in Tabasco México, have in their composition, two different crystalline structures: calcite in superior percentage and traces of aragonite. Due to their biogenic origin, they contain amide groups. These crystalline phases, are modified in content by thermal annealing effect of WOS at 500 °C because the aragonite is transformed into calcite by the annealing treatment in a 100%. When waste oyster shell powders are subjected to thermal treatments of 700 and 900°C, calcite is transformed into $Ca(OH)_2$ (portlandite). Results of characterization techniques by XRD, SEM and HRTEM show that it is possible to obtain nanostructured $CaCO_3$ from waste oyster shells, with 200 nm particle size and well-defined crystalline structures (orthorhombic and rhombohedral phase). These phase transitions are evident with the size decrease to 40 nm and regular shape of particles at 500 °C. Waste oyster shell is a biogenic material that can be used as a precursor material of nanostructured $CaCO_3$ for industrial uses. On the other hand, it is possible to use the portlandite obtained in the hexagonal phase of $Ca(OH)_2$, with thermal treatment at 700 °C, as a restoring material for old buildings. Besides, with a thermal treatment at 900 °C, high purity $Ca(OH)_2$ is obtained, although 67% yield was reached, after being under grinding and thermal annealing processes, $Ca(OH)_2$ becomes feasible in commercialization as a chemical reactive precursor.

Acknolwedgements

We would like to thank CONACYT for granting the scholarship 582381 to Candelario Ramón de los Santos and the project INFRA -2014 -225962 funded by CONACYT. Ing. Saúl García López for assistance with HRTEM imaging in the UJAT CICTAT for TEM measurements.

References

1. Yu, Y.; Smyth J. R.; Bon, P. *American Mineralogist*. **2012**, *97*, 707–712. DOI: http://dx.doi.org/10.2138/am.2012.3923
2. Yoshioka S.; Kitano Y. *Geochemical Journal.* **1985**, 19, 245 to 249. DOI: https://doi.org/10.2343/geochemj.19.245
3. Manjusha, H.; Neethumol, V.; Benny, C. A.; Sreenivasan P.V.; Jenish, P.; Asmy, A.K.A, *International Journal of Scientific and Research Publications.* **2014**, 4, 10. ISSN 2250-3153
4. Checa, A.G.; Esteban-Delgado, F.J.; Rodrıíguez-Navarro, A.B. *Journal of Sctructural Biology.* **2007**, *157,* 393–402. DOI:10.1016/j.jsb.2006.09.005
5. Hamester, M.R.R.; Balzer, P.S.; Becker, D. *Materials Research.* **2012***, 15,* 204-208. DOI: http://dx.doi.org/10.1590/S1516-14392012005000014
6. Chen Y.; Lian X.; Li Z.; Zheng S., Wang Z., Advanced Powder Technology, **2015**, 26, 505-510. DOI: http://dx.doi.org/10.1016/j.apt.2014.12.007
7. Bastida J., Bolós C., Pardo P., Serrano F. J., Bol. Soc. Esp. Ceram. V. **2004**, 43, 80-83. DOI: 10.3989/cyv.2004.v43.i1.621
8. Yoon, G.L.; Kim, B.T.; Kim, B.O.;Han, S.H. *Waste Managment,* **2003**, *23,* 825-34. DOI: 10.1016/S0956-053X(02)00159-9
9. Yong, S. O.; Sang Eun, O.; Mahtab, A.; Hyun, S.; Kwon Rae, K.; Deok Hyun, M.; Sang Soo, L.; Kyoung Jae, L.; Weon Tai, J.; Jae E, Y. *Environ Earth Science.* **2010***, 61,*1301-1308. DOI 10.1007/s12665-010-0674-4
10. Lee, C.W.; Kwon, H.B.; Jeon, H.P.; Koopman, B. *Journal Clean Production.* **2009***, 17,*683–687. DOI : 10.1016/j.jclepro.2008.11.019
11. Jae-Hoon Huh, Young-Hoon Choi*, Chilakala Ramakrishna, Sun Hee Cheong** and Ji Whan Ahn Jae-Hoon, H., Young-Hoon, C., Chilakala, R., Sun Hee, C., Ji Whan, A. *Journal of the Korean Ceramic Society.* **2016**, 53, 429-434. DOI: http://dx.doi.org/10.4191/kcers.2016.53.4.429.
12. Khan, MD., Ahn, JW., Nam, G. Journal of Environmental Management. **2018**, 223, 947-951. DOI: 10.1016/j.jenvman.2018.07.011

J. Mex. Chem. Soc. **2019**, *63*(1)

ISSN-e 2594-0317

13. Weiner, S., Mahamid, J., Politi, Y., Ma, Y., Addadi, L. Frontiers of Materials Science in China. **2009**, 3, 104. DOI: 10.1007/s11706-009-0036-x.
14. Cartwright, J.H. E., Checa, A.G., Gale, J.D., Gebauer, D., Sainz-Díaz, C. I. Angewandte Chemie. **2012**, 51, 11960-11970. DOI: https://doi.org/10.1002/anie.201203125.
15. Kladi A., Klepetsanis P.G., Østvold T., Kontoyiannis C.G., Koutsoukos P.G. *Advances in Crystal Growth Inhibition Technologies***. 2002**, Springer, Boston, MA. DOI: 10.1.1.846.4070&rep=rep1&type=pdf
16. Chiou I.J., Chen C.H., Li Y.H. Construction and Building Materials. **2014**, 64, 480-487. DOI: http://dx.doi.org/10.1016/j.conbuildmat.2014.04.101
17. Ramon de los Santos, C., Barajas Fernandez, J., Perez Hernandez, G., Hernandez Rivera, M.A., Diaz Flores, L.L. Bol. Soc. Esp. Cerám. Vidr. **2018**, https://doi.org/10.1016/j.bsecv.2018.05.003
18. Yong, S. O., Jung, E. L., Deok, H. M. *Environ Geochem Health*. **2011**, 33,83-91. DOI 10.1007/s10653-010-9329-3
19. Islam, K.N.; Abu Bakar, Z.B.; Ali, E.; Bin Hussein, M.Z.; Noordin, M.M.; Loqman, M.Y.; Miah, G.; Wahid, H.; Hashim, U. *Powder Technology.* ***2013****,235,* 70-75. DOI: https://doi.org/10.1016/j.powtec.2012.09.041
20. Yash, B.; Vishnu, K. P.; Jian, L.*Journal of Materials Chemistry.* **2016**, *2,*14270-14288. DOI:10.1039/C4TA02070G
21. Shan-Yang, L.; Mei-Jane, L.;Wen-Ting, C. *Spectroscopy.* **2007**, *21,* 1-30. DOI: http://dx.doi.org/10.1155/2007/278765
22. Yousefpour, M.; Askari, N.; Abdollah-Pour, H. *Biotechnology and Biomaterials.* **2011***, 1,*1-4. DOI:10.4172/2155-952X.1000105
23. Vagenas, N.V.; Gatsouli, A.;Kontoyannis, C.G. *Talanta.* **2003**, *10,* 831-836. DOI: 10.1016/S0039-9140(02)00638-0.
24. Rodríguez-Navarro, C.; Elert, K.; Sevcik, R. *Cryst. Eng. Comm.* **2016**, *18,* 6594-6607. DOI:10.1039/C6CE01202G